

# Finite-size scaling relations of the four-dimensional Ising model on the Creutz cellular automaton

Z. Merdan and E. Güzelsoy

*Kirikkale University, Faculty of Arts and Sciences, Department of Physics, Yahşihan 71250, Kirikkale, Turkey*  
E-mail: zmerdan1967@hotmail.com

Received August 28, 2010

The four-dimensional Ising model is simulated on the Creutz cellular automaton using the finite-size lattices with the linear dimension  $4 \leq L \leq 8$ . The temperature variations and the finite-size scaling plots of the specific heat and the Binder parameter verify the theoretically predicted expression near the infinite lattice critical temperature for the 7, 14, and 21 independent simulations. The approximate values for the critical temperature of the infinite lattice,  $T_c(\infty) = 6.6965(35)$ ,  $6.6961(30)$ ,  $6.6960(12)$ ,  $6.6800(3)$ ,  $6.6801(2)$ ,  $6.6802(1)$  and  $6.6925(22)$  (without logarithmic factor),  $6.6921(22)$  (without logarithmic factor),  $6.6909(2)$  (without logarithmic factor),  $6.6822(13)$  (with logarithmic factor),  $6.6819(11)$  (with logarithmic factor),  $6.6808(8)$  (with logarithmic factor) are obtained from the intersection points of specific heat curves, the Binder parameter curves and the straight line fit of specific heat maxima for the 7, 14, and 21 independent simulations, respectively. As the number of independent simulations increases, the obtained results,  $6.6802(1)$  and  $6.6808(8)$ , are in very good agreement with the series expansion results of  $T_c(\infty) = 6.6817(15)$ ,  $6.6802(2)$ , the dynamic Monte Carlo result of  $T_c(\infty) = 6.6803(1)$ , the cluster Monte Carlo result of  $T_c(\infty) = 6.680(1)$  and the Monte Carlo using Metropolis and Wolff-cluster algorithm of  $T_c(\infty) = 6.6802632 \pm 5 \cdot 10^{-5}$ . The average values obtained for the critical exponent of the specific heat are calculated as  $\alpha = -0.0402(15)$ ,  $-0.0393(12)$ ,  $-0.0391(11)$  for the 7, 14, and 21 independent simulations, respectively. As the number of independent simulations increases, the obtained result,  $\alpha = -0.0391(11)$ , is agreement with the series expansions results of  $\alpha = -0.12 \pm 0.03$  and the Monte Carlo using Metropolis and Wolff-cluster algorithm of  $\alpha \geq 0 \pm 0.04$ . However,  $\alpha = -0.0391(11)$  isn't consistent with the renormalization group prediction of  $\alpha = 0$ .

PACS: **05.45.-a** Computational methods in statistical physics and nonlinear dynamics;  
75.10.Hk Classical spin models;  
75.40.Cx Static properties.

Keywords: Ising model, cellular automata, critical exponents, finite-size scaling.

## 1. Introduction

While the four-dimensional Ising model is not directly applicable to real magnetic systems, it is useful to investigate the influence of dimensionality on phase transitions [1]. In fact, in Euclidean quantum field theory the 4D Ising model describes the physical dimension. As the dimension and/or the lattice size increases, the simulation of the Ising model by the conventional Monte Carlo method becomes impractical and faster algorithms are needed. The Creutz cellular automaton [2] does not require high-quality random numbers, is an order of magnitude faster than the conventional Monte Carlo method, and compared to the Q2R cellular automaton [3], and also has the advantage of fluctuating internal energy from which the specific heat can be computed.

The purpose of this study is to the finite-size scaling relations for the specific heat and the Binder parameter near the infinite-lattice critical temperature in  $d = 4$  dimensions on the Creutz cellular automaton for the 7, 14, and 21 independent simulations. The critical temperatures for the specific heat and the Binder parameter and static critical exponents for the specific heat are obtained by analyzing the data within the framework of the renormalization group theory [4,5] either by approximating the infinite lattice by suitable finite-size lattice [6] or by using the finite-size scaling relations available [7–9].

The simulations are carried out on the Creutz cellular automaton [2,10] which has arisen as an alternative research tool for Ising model investigations and has simulated the Ising model in the dimensionalities  $2 \leq d \leq 8$  [11,12].

This paper is organized as follows. The model is described in Sec. 2, the results are discussed in Sec. 3, and a conclusion is given in Sec. 4.

### 2. Model

Five binary bits are associated with each site of the lattice. The value for each site is determined from its value and those of its nearest neighbors at the previous time step. The updating rule, which defines a deterministic cellular automaton, is as follows. Of the five binary bits on each site, the first one is the Ising spin  $B_i$ . Its value may be “0” or “1”. Ising spin energy (internal energy) of the lattice,  $H_I$ , is given (in units of the nearest neighbor coupling constant  $J$ ) by

$$H_I = -J \sum_{\langle i,j \rangle} S_i S_j, \tag{1}$$

where  $S_i = 2B_i - 1$  and  $\langle i, j \rangle$  denotes the sum over all nearest neighbor pairs of sites. The next three bits are for the momentum variable conjugate to the spin (the demon). These three bits form an integer which can take on the values within the interval (0,7). The kinetic energy (in units of  $J$ ) associated with the demon can take on four times these integer values. The total energy

$$H = H_I + H_K \tag{2}$$

is conserved; here  $H_K$  denotes the kinetic energy of the lattice. For a given total energy the system temperature  $T$  (in units of  $J/k_B$  where  $k_B$  is the Boltzmann constant) is obtained from the average value of the kinetic energy. The fifth bit provides a checkerboard style updating, and so it allows the simulation of the Ising model on a cellular automaton. The black sites of the checkerboard are updated and then their colour is changed into white: the white sites are changed into black without being updated.

The updating rules for the spin and the momentum variables are as follows: for a site to be updated its spin is flipped and the change in the Ising energy (internal energy),  $H_I$ , is calculated. If this energy change is transferable to or from the momentum variable associated with this site, such that the total energy,  $H$ , is conserved, then this change is done and the momentum is appropriately changed. Otherwise the spin and the momentum are not changed.

As the initial configuration all the spins are taken ordered (up or down). The initial kinetic energy is given to the lattice via the third bits of the momentum variables in the white sites randomly, such that the value of the initial kinetic energy for such a demon is 16 (in units of  $J$ ) which is just the amount need to flip a spin at its initial configuration.

The simulations are carried out on simple hypercubic lattices  $L^4$  of linear dimensions  $4 \leq L \leq 8$  with periodic boundary conditions by using four-bit demons. The cellular automaton develops  $9.6 \cdot 10^5$  ( $L = 4, 6, 8$ ) sweeps for each run with 7, 14, and 21 runs for each total energy

which total energy is average arithmetic for 7, 14, and 21 runs.

### 3. Results and discussion

The temperature-dependence of the functions for the specific heat ( $C_L$ ) and the Binder parameter ( $g_L$ ) using the finite-size lattice with the linear dimension  $4 \leq L \leq 8$  are illustrated in Figs. 1 and 2 for 7, 14, and 21 independent simulations. The finite-size lattice critical temperatures obtained from the specific heat maxima  $T_c^C(L)$  and the intersection points of specific heat curves are listed in Table 1. The singular part of the free-energy density  $f_L^S(t, h)$  of a hypercubic finite system  $L^d$  with periodic boundary conditions for  $d < d_u$  is given by Privman and Fisher [13] as

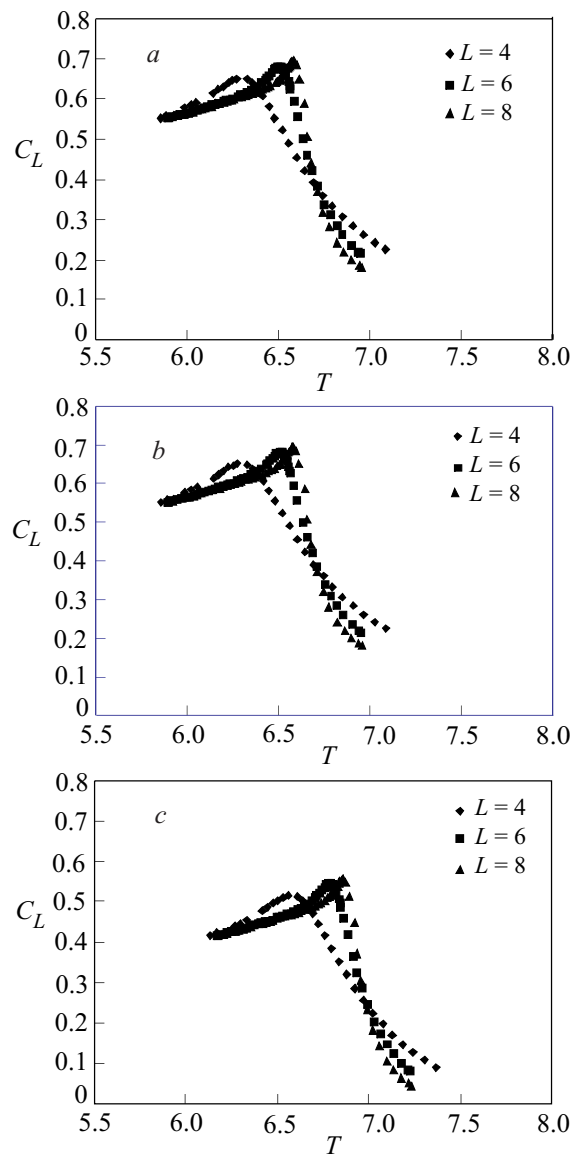


Fig. 1. The temperature-dependence of the specific heat  $C_L$  for 7 (a), 14 (b) and 21 (c) independent simulations ( $4 \leq L \leq 8$ ).

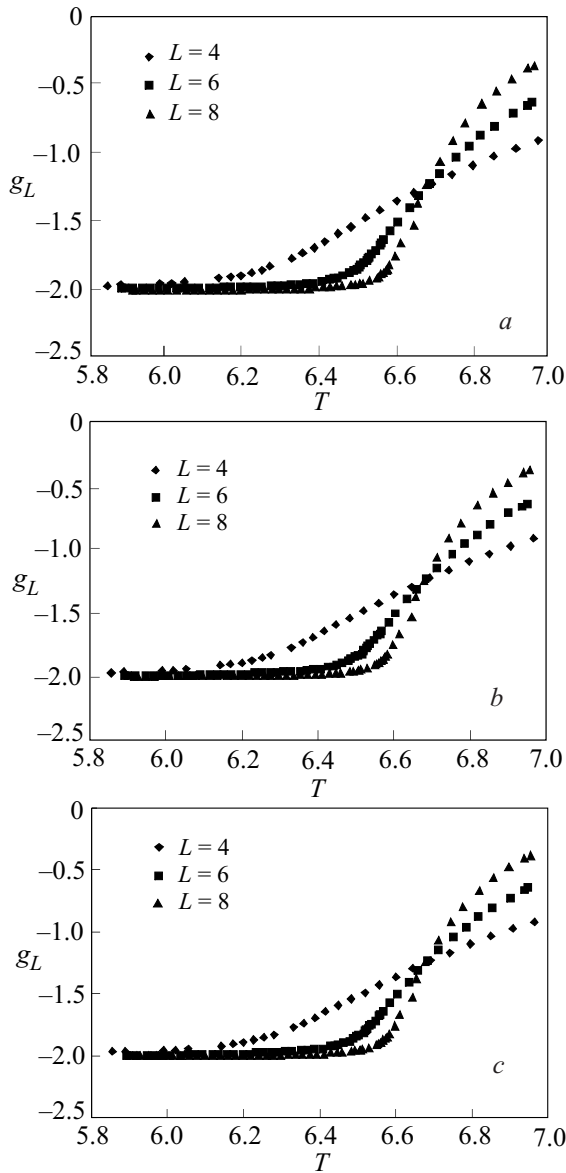


Fig. 2. The temperature-dependence of the Binder parameter  $g_L$  for 7 (a), 14 (b) and 21 (c) independent simulations ( $4 \leq L \leq 8$ ).

$$f_L^{(S)}(t, h) = L^{-d} Y(C_1 t L^{1/\nu}, C_2 h L^\Delta), \quad (3)$$

$$t \rightarrow 0, \quad h \rightarrow 0, \quad L \rightarrow \infty,$$

where  $\Delta$  is the gap exponent,  $\nu$  is critical exponent for the correlation length for the infinite system,  $t = (T - T_c)/T_c$  is the reduced temperature,  $d_u$  is the upper critical dimension and  $h$  is the reduced external magnetic field. The scale factors  $C_1$  and  $C_2$  are the only nonuniversal system-dependent parameters, that is, the scaling function  $Y(x, y)$  is universal, with no further nonuniversal prefactor.

The Privman–Fisher hypothesis for the singular part of the free-energy density  $f_L^S(t, h)$  of a hypercubic finite system  $L^d$  with periodic boundary conditions is adapted for the Ising model in  $d = 4$  dimension [11], by proposing

the finite-size scaling function  $Y(x, y)$ , correct to leading logarithms, as below:

$$f_L^{(S)}(t, h) = L^{-d} Y(C_1 t L^2 \log^{1/6} L, C_2 h L^3 \log^{1/4} L), \quad (4)$$

$$t \rightarrow 0, \quad h \rightarrow 0, \quad L \rightarrow \infty.$$

Table 1. The values of  $T_c^C(L)$  (the finite-size lattice critical temperatures obtained from the specific heat maxima),  $C_L^{\max}$  and  $C_L(T_c)$  (at  $T_c = 6.6802(2)$ ) for 7, 14, and 21 independent simulations

The number of independent simulations	$L$	$T_c^C(L)$	$C_L^{\max}$	$C_L(T_c)$
7	4	6.2748(6)	0.6509(10)	0.3994(78)
		6.2758(8)	0.6508(15)	0.3995(52)
		6.2792(8)	0.6511(16)	0.3992(17)
14	6	6.5163(8)	0.6806(18)	0.4266(61)
		6.5164(6)	0.6803(21)	0.4268(38)
		6.5167(6)	0.6802(20)	0.4269(15)
21	8	6.5823(8)	0.6952(32)	0.4406(52)
		6.5824(3)	0.6951(26)	0.4405(21)
		6.5827(4)	0.6949(25)	0.4402(11)

From Eq. (4) the finite-size scaling expressions for the singular part of the specific heat  $C_L^{(S)}(t, h)$  can be derived as

$$C_L^{(S)}(t, h) = -\frac{\partial^2 f_L}{\partial t^2} =$$

$$= \log^{1/3}(L) C_1^2 W(C_1 t L^2 \log^{1/6} L, C_1 h L^3 \log^{1/4} L). \quad (5)$$

It can be rewritten in more informative form as follow:

$$C_L^{(S)}(t, h) = L^{\alpha/\nu} \log^{1/3}(L) C_1^2 \times$$

$$\times W(C_1 t L^2 \log^{1/6} L, C_2 h L^3 \log^{1/4} L), \quad \alpha = 0, \quad (6)$$

where  $\alpha$  is the critical exponent for the specific heat;  $W$  is the corresponding finite-size scaling function. For  $h = 0$ , it reduces to the following equation:

$$C_L^{(S)}(t) = L^{\alpha/\nu} \log^{1/3}(L) C_1^2 W(C_1 t L^2 \log^{1/6} L), \quad \alpha = 0. \quad (7)$$

For  $h = 0$  and  $t = 0$  it reduces to

$$C_L^{(S)}(t) = L^{\alpha/\nu} \log^{1/3}(L) C_1^2 W(0, 0), \quad \alpha = 0. \quad (8)$$

$W(0, 0)$  is universal. The Eq. (6) for  $h = 0$  can be tested by simulations directly for 7, 14, and 21 independent simulations.

In Fig. 3, we show the finite-size scaling plots of the specific heat for 7, 14, and 21 independent simulations. In this figure, not all of the data points for a given  $L$  fall on the finite-size scaling curve. Since not all the scaled quantities of  $C_L$  for the different  $L$  values overlap, the finite-size scaling relation for  $C_L$  is verified near the reduced

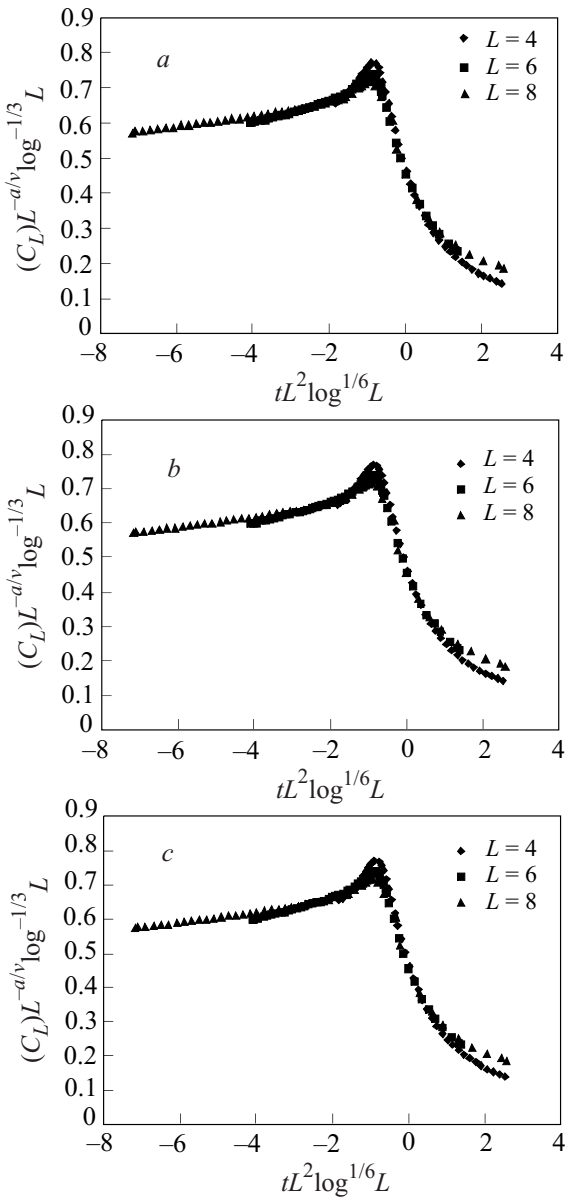


Fig. 3. Finite-size scaling plots of the specific heat  $C_L$  with  $\alpha/\nu=0$  at  $T_c = 6.6802(2)$  for 7 (a), 14 (b) and 21 (c) independent simulations.

temperature ( $t = (T - T_c)/T_c$ ) for 7, 14, and 21 independent simulations. It should be mentioned that the contribution of  $C_L$  from the regular part is not considered in this plot. That is, the values of the specific heat computed in the simulations are used directly in the plots.

The dependences of the critical temperature  $T_c^C(L)$  obtained from the specific heat maxima of the finite-size lattices on the linear dimension ( $L$ ) are given by the following relations [7]:

$$T_c^C(\infty) - T_c^C(L) \propto L^{-1/\nu}, \tag{9}$$

$$T_c^C(\infty) - T_c^C(L) \propto L^{-1/\nu} \log^{-1/6} L. \tag{10}$$

The finite-size critical temperatures,  $T_c^C(L)$ , are plotted without and with logarithmic factors for 7, 14 and 21 independent simulations. For both cases the straight lines which fit to these data give  $T_c(\infty) = 6.6925(22)$ ,  $6.6921(22)$ ,  $6.6909(2)$  and  $T_c(\infty) = 6.6822(13)$ ,  $6.6819(11)$ ,  $6.6808(8)$  without and with logarithmic factors for 7, 14, and 21 independent simulations, respectively (Table 2). The intersection of the curves in Fig. 1 for  $4 \leq L \leq 8$  gives the critical temperatures of  $T_c(\infty) = 6.6965(35)$ ,  $6.6961(30)$ ,  $6.6960(12)$  for 7, 14, and 21 independent simulations, respectively (Table 2). As the number of independent simulations increases, the obtained result,  $T_c(\infty) = 6.6808(8)$  (with logarithmic factors) is consistent with the series expansion results of  $T_c(\infty) = 6.6817(15)$  [14],  $T_c(\infty) = 6.6802(2)$  [15], the dynamic Monte Carlo result of  $T_c(\infty) = 6.6803(1)$  [15], the cluster Monte Carlo result of  $T_c(\infty) = 6.680(1)$  [9], the Creutz cellular automaton results of  $T_c(\infty) = 6.680, 6.6802(2), 6.682$  and  $6.67$  [11,12] and the Monte Carlo using Metropolis and Wolff-cluster algorithm of  $T_c(\infty) = 6.6802632 \pm 5 \cdot 10^{-5}$  [16].

Table 2. The values of critical temperatures for the infinite lattice obtained from by fitting the data for the critical temperatures  $T_c^C(L)$  (without logarithmic factor) and  $T_c^C(L)$  (with logarithmic factor) within the interval  $4 \leq L \leq 8$  for 7, 14, and 21 independent simulations

The number of independent simulations	$T_c^C(\infty)$ (without logarithmic factor)	$T_c^C(\infty)$ (with logarithmic factor)	$T_c(\infty)$ (the intersection points of specific heat curves)
7	6.6925(22)	6.6822(13)	6.6965(35)
14	6.6921(22)	6.6819(11)	6.6961(30)
21	6.6909(2)	6.6808(8)	6.6960(12)

The dependence of the specific heat  $C(L)$  on the linear dimension  $L$  of the finite-size lattices is given by the relation [7,9]

$$C(L) \propto L^{\alpha/\nu} \log^{1/3} L, T_c(\infty), T_c^C(L). \tag{11}$$

The values of the specific heat ( $C_L^{\max}$  and  $C_L(T_c)$ ) obtained from Fig. 1 for the finite-size lattices with the linear dimensions  $4 \leq L \leq 8$  are listed in Table 1. The values of  $[\alpha/\nu]_{\max}$  and  $[\alpha/\nu]_c$  obtained according to Eq. (11) for the finite-lattice at the infinite-lattice critical temperatures are  $[\alpha/\nu]_{\max} = -0.1001(0), -0.1001(1), -0.1012(2)$ ,  $[\alpha/\nu]_c = -0.0530(38), -0.0536(58), -0.0534(11)$  for 7, 14, and 21 independent simulations using lattices with the linear dimension  $4 \leq L \leq 8$ , respectively (Table 3). The values of the critical exponents  $\alpha_{\max}$  and  $\alpha_c$  with  $\nu = 1/2$  are computed to be  $\alpha_{\max} = -0.0530(16), -0.0513(13), -0.0512(12)$  and  $\alpha_c = -0.0273(14), -0.0272(11), -0.0269(10)$  for 7, 14, and 21 independent simulations, respectively. The average values of  $\alpha_{\max}$  and  $\alpha_c$  for 7, 14, and 21 independent simulations are

Table 3. The values of critical exponents  $[\alpha/v]_{\max}$ ,  $[\alpha/v]_c$ ,  $\alpha_{\max}$ ,  $\alpha_c$ ,  $\alpha_{\text{average}}$  for the set of finite-size lattices within the interval  $4 \leq L \leq 8$  for 7, 14 and 21 independent simulations

The number of independent simulations	$[\alpha/v]_{\max}$	$[\alpha/v]_c$	$\alpha_{\max}$	$\alpha_c$	$\alpha_{\text{average}}$
7	-0.1001(0)	-0.0530(38)	-0.0530(16)	-0.0273(14)	-0.0402(15)
14	-0.1001(1)	-0.0536(58)	-0.0513(13)	-0.0272(11)	-0.0393(12)
21	-0.1012(2)	-0.0534(11)	-0.0512(12)	-0.0269(10)	-0.0391(11)

$\alpha_{\text{average}} = -0.0402(15)$ ,  $-0.0393(12)$ ,  $-0.0391(11)$ , respectively (Table 3). As the number of independent simulations increases, the obtained result,  $\alpha_{\text{average}} = -0.0402(15)$ , is consistent with the series expansions results of  $\alpha = -0.12 \pm 0.03$  [17], the Creutz cellular automaton results of  $\alpha = -0.04$  and  $-0.018$  [11,12] and the Monte Carlo using Metropolis and Wolff-cluster algorithm of  $\alpha \geq 0 \pm 0.04$  [16] within the error limits. However,  $\alpha = -0.0391(11)$  isn't consistent with the renormalization group prediction of  $\alpha = 0$ .

The  $h=0$  finite size renormalized coupling  $g_L$  (Binder parameter or Binder cumulant) introduced by Binder [18]

$$g_L = \frac{\langle s^4 \rangle_L}{\langle s^2 \rangle_L^2} - 3 = \left[ \frac{\chi_L^{(4)}}{L^4 \chi_L^4} \right]_{h=0}, \quad (12)$$

where  $\chi_L$  is the susceptibility and  $\chi_L^{(4)}$  is the fourth field derivate; the subscripts  $L$  denotes the corresponding finite-size quantities. In the method of Binder [18], the critical point  $T_c$  is located by finding the common crossing point of plots of  $g_L$  versus temperature for a range of different system sizes  $L$ . The temperature variations of the Binder parameter for  $L=4, 6$  and  $8$  are shown in Fig. 2 for 7, 14, and 21 independent simulations. In this figure, the intersection points of the curves for  $4 \leq L \leq 8$  give  $T_c = 6.6800(3)$ ,  $6.6801(2)$ ,  $6.6802(1)$  for 7, 14, and 21 independent simulations. As the number of independent simulations increases, the obtained result,  $T_c = 6.6802(1)$ , is consistent with the series expansion results of  $T_c(\infty) = 6.6817(15)$  [14],  $6.6802(2)$  [15], the dynamic Monte Carlo result of  $T_c(\infty) = 6.6803(1)$  [15], the cluster Monte Carlo result of  $T_c(\infty) = 6.680(1)$  [9], the Creutz cellular automaton results of  $T_c(\infty) = 6.680$ ,  $6.6802(2)$ ,  $6.682$  and  $6.67$  [11,12] and the Monte Carlo using Metropolis and Wolff-cluster algorithm of  $T_c(\infty) = 6.6802632 \pm 5 \cdot 10^{-5}$  [16]. The computed values of  $g_L(T_c)$  for  $L=4, 6$  and  $8$  are listed in Table 4 for 7, 14, and 21 independent simulations. By using the data in Table 4 in getting plots of  $g_L(T_c)$  vs.  $L$ , the following of values  $g_L(T_c)$  are obtained:  $g_L(T_c) = -1.25(43)$ ,  $-1.22(25)$ ,  $-1.24(5)$  for 7, 14, and 21 independent simulations, respectively (Table 5). As the number of independent simulations increases, the obtained result,  $g_L(T_c) = -1.24(5)$ , is inconsistent with the Monte Carlo simulations results of  $g_L(T_c) \cong -1.08$  for size  $L=14$  [19], the analytic prediction

of  $g_L(T_c) \cong -0.81156$  by Brezin and Zinn-Justin [20], the Creutz cellular automaton results of  $g_L = -0.8$  for  $L=14$  [11], the geometrical cluster Monte Carlo method results of  $g_L = -0.830(2)$  [21].

 Table 4. The values of  $g_L(T_c)$  obtained from the finite-size lattices for 7, 14, and 21 independent simulations at the infinite-lattice critical temperature

The number of independent simulations	$L$	$g_L(T_c)$
7	4	-1.2456(39)
14		-1.2317(36)
21		-1.2410(28)
7	6	-1.2466(35)
14		-1.2473(32)
21		-1.2388(24)
7	8	-1.2464(31)
14		-1.2473(24)
21		-1.2378(15)

 Table 5. The values of  $T_c(\infty)$  and  $g_L(T_c)$  obtained from intersection points of the Binder parameter curves for 7, 14, and 21 independent simulations ( $4 \leq L \leq 8$ )

The number of independent simulations	$g_L(T_c)$	$T_c(\infty)$ (the intersection points of Binder parameter curves)
7	-1.25(43)	6.6800(3)
14	-1.22(25)	6.6801(2)
21	-1.24(5)	6.6802(1)

From Eq. (4) the finite-size scaling expression for the Binder Cumulant [11],  $g_L(t, h)$ , can be derived as

$$g_L(t, h) = \frac{\chi_L^{(4)}}{L^4 \chi_L^2} = G(C_1 t L^2 \log^{1/6} L, C_2 h L^3 \log^{1/4} L), \quad (13)$$

with the fourth derivative given by  $\chi_L^{(4)} = -\partial^2 f_L / \partial h^4$ . For  $h=0$  Eq. (13) reduce to the following equation:

$$g_L(t) = G(C_1 t L^2 \log^{1/6} L). \quad (14)$$

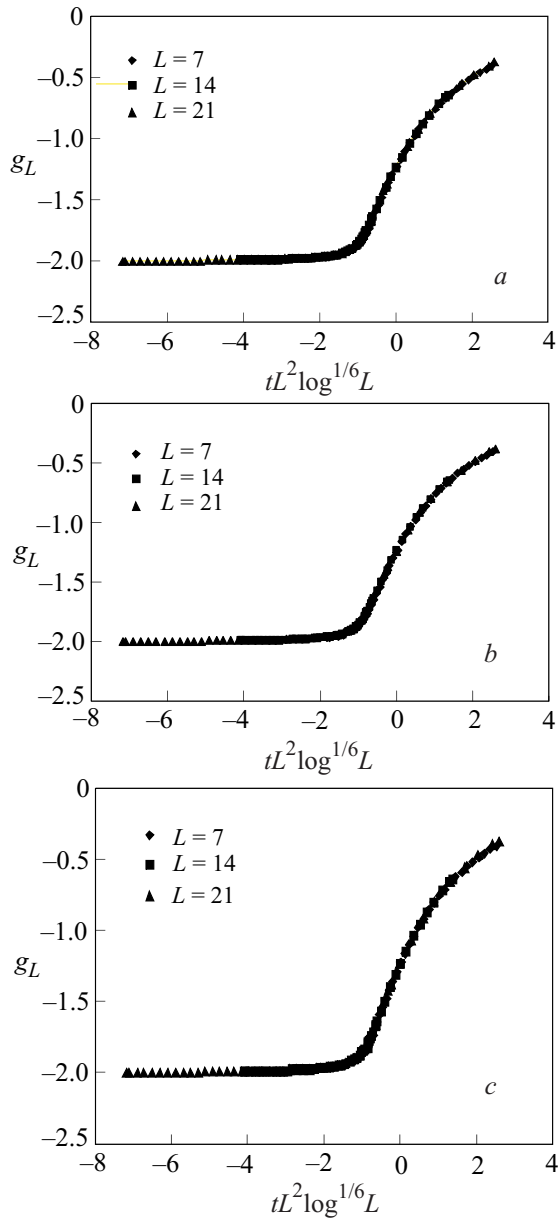


Fig. 4. Finite-size scaling plots of the Binder parameter  $g_L$  at  $T_c = 6.6802(2)$  for 7 (a), 14 (b) and 21 (c) independent simulations.

For  $h = 0$ ,  $t = 0$  Eq. (13) reduces to the following equation:

$$g_L(t) = G(0, 0). \quad (15)$$

$G(0, 0)$  is universal. The Eq. (14) for  $h = 0$  can be tested by simulations directly for 7, 14, and 21 independent simulations.

The finite-size scaling plot of the Binder parameter at  $T_c(\infty) = 6.6802(2)$  is illustrated in Fig. 4 for 7, 14, and 21 independent simulations. The finite-size scaling plot of the Binder parameter for 7, 14, and 21 independent simulations is a complete overlap of the plots for different  $L$ , verifying the finite-size scaling relation given Eq. (14).

#### 4. Conclusions

The Ising model in  $d = 4$  dimension is simulated on the Creutz cellular automaton using the finite-size lattice with the linear dimensions  $4 \leq L \leq 8$ . As the number of simulations increases, the exponent obtained by finite-size scaling relation for the specific heat at the infinite-lattice critical temperature,  $\alpha = -0.0391(11)$ , is consistent with the series expansions results of  $\alpha = -0.12 \pm 0.03$ , the Creutz cellular automaton results of  $\alpha = -0.04$ ,  $-0.018$  and the Monte Carlo using Metropolis and Wolff-cluster algorithm of  $\alpha \geq 0 \pm 0.04$  [16] within the error limits. However,  $\alpha = -0.0391(11)$  isn't consistent with the renormalization group prediction of  $\alpha = 0$ , since not all the scaled quantities of  $C_L$  for the different  $L$  values overlap, the finite-size scaling relation for  $C_L$  is verified near the reduced temperature ( $t = (T - T_c) / T_c$ ) for 7, 14, and 21 independent simulations. On the other hand, since all the scaled quantities of  $g_L$  for the different  $L$  values overlap at the infinite-size critical temperature, the finite-size scaling relation for  $g_L$  is verified for 7, 14, and 21 independent simulations.

1. H.W.J. Blöte and R.H. Swendsen, *Phys. Rev.* **B22**, 4481 (1980).
2. M. Creutz, *Ann. Phys.* **167**, 62 (1986).
3. W.M. Lang and D. Stauffer, *J. Phys.* **A20**, 5413 (1987).
4. A.I. Larking and D.E. Khmel'nitskii, *Zh. Eksp. Teor. Fiz.* **56**, 2087 (1969) [*Sov. Phys. JETP* **29**, 1123 (1969)].
5. E. Brezin, J.C. Le Guillou, and J. Zinn-Justin, *Phys. Rev.* **D8**, 2418 (1973).
6. O.G. Mouritsen and S.J. Knak Jensen, *Phys. Rev.* **B19**, 3663 (1979); O.G. Mouritsen and S.J. Knak Jensen, *J. Phys.* **A12**, L 339 (1979).
7. J. Rudnick, H. Guo, and D. Jasnow, *J. Stat. Phys.* **41**, 353 (1985); D. Jasnow, in: V. Privman (ed.), *Finite-Size Scaling and Numerical Simulation of Statistical Systems*, World Scientific, Singapore (1990), p. 99.
8. V. Privman (ed.), *Finite-Size Scaling and Numerical Simulation of Statistical Systems*, World Scientific, Singapore (1990).
9. R. Kenna and C.B. Lang, *Phys. Lett.* **B264**, 396 (1991); R. Kenna and C.B. Lang, *Nucl. Phys.* **B393**, 461 (1993).
10. N. Aktekin, in: D. Stauffer (ed.), *Annual Reviews of Computational Physics*, Vol. VII, World Scientific, Singapore (2000), p. 1.
11. B. Kutlu and N. Aktekin, *Physica* **A208**, 423 (1994); N. Aktekin, *Physica* **A219**, 436 (1995); B. Kutlu, *Physica* **A234**, 807 (1997); B. Kutlu, *Physica* **A243**, 199 (1997); N. Aktekin, *Int. J. Mod. Phys.* **C8**, 287 (1997); N. Aktekin, *Phys.* **A232**, 397 (1996); N. Aktekin, *J. Stat. Phys.* **232**, 397 (1996); N. Aktekin, A. Günen, and Z. Sağlam, *Int. J. Mod. Phys.* **C10**, 875 (1999); N. Aktekin, Ş. Erkoç, and M. Kalay, *Int. J. Mod. Phys.* **C10**, 1237 (1999); N. Aktekin and Ş. Erkoç, *Physica* **A284**, 206 (2000); N. Aktekin, *J. Stat. Phys.*

- 104**, 1397 (2001); N. Aktekin and Ş. Erkoç, *Physica* **A290**, 123 (2001).
12. Z. Merdan and R. Erdem, *Phys. Lett.* **A330**, 403 (2004); Z. Merdan and M. Bayirli, *Appl. Math. and Comp.* **167**, 212 (2005); Z. Merdan, A. Günen, and G. Mülazimoğlu, *Int. J. Mod. Phys.* **C16**, 269 (2005); Z. Merdan, A. Duran, D. Atille, G. Mülazimoğlu, and A. Günen, *Physica* **A366**, 265 (2006); Z. Merdan, A. Günen, and Ş. Çavdar, *Physica* **A359**, 415 (2006); Z. Merdan and D. Atille, *Physica* **A376**, 327 (2007); Z. Merdan and D. Atille, *Mod. Phys. Lett.* **B21**, 215 (2007); G. Mülazimoğlu, A. Duran, Z. Merdan, and A. Günen, *Mod. Phys. Lett.* **B22**, 1329 (2008); Z. Merdan, M. Bayirli, and M.K. Öztürk, *Z. Naturforsch.* **A64**, 1 (2009); Z. Merdan, M. Bayirli, and M.K. Öztürk, *Z. Naturforsch.* **A65**, 705 (2010); Z. Merdan, M.K. Öztürk, C. Kürkçü, and A. Günen, *Journal of Optoelectronics and Advanced Materials-Symposia* **1**, 205 (2009).
13. V. Privman and M.E. Fisher, *Phys. Rev.* **B30**, 322 (1984); V. Privman, in *Finite-Size Scaling and Numerical Simulation of Statistical Systems*, V. Privman (ed.), World Scientific, Singapore (1990), p. 1.
14. D.S. Gaunt, M.F. Sykes, and S. McKenzie, *J. Phys.* **A12**, 871 (1979).
15. D. Stauffer and J. Adler, *Int. J. Mod. Phys.* **C8**, 263 (1997).
16. P.H. Lundow and K. Markström, *Phys. Rev.* **E80**, 031104 (2009).
17. M.A. Moore, *Phys. Rev.* **B1**, 2238 (1970).
18. K. Binder, M. Nauenberg, V. Privman, and A.P. Young, *Phys. Rev.* **B31**, 1498 (1985).
19. P.-Y. Lai and K.K. Mon, *Phys. Rev.* **B41**, 9257 (1990).
20. E. Brezin and J. Zinn-Justin, *Nucl. Phys.* **B257**, 867 (1985).
21. J.R. Heringa, H.W.J. Blöte, and E. Luijten, *J. Phys.* **A33**, 2929 (2000).